CHAPTER 2

THEORETICAL DETAILS

This chapter gives a brief introduction to the ion conduction mechanism in polymer electrolytes and the applicability of different theoretical models to polymer electrolytes. Also, various conductivity formalism has been described in detail.

2.1 Introduction

The polymer electrolytes contain both crystalline and amorphous phases along with the association of charge carriers, which is an example of disordered material [1]. Hence, the electrical conduction mechanism or ion transport behavior is a challenging task. The ionic transport mechanism in polymer electrolytes is quite different from that occurring in liquid electrolytes. Ion transport in liquid and solid is a consequence of random migration of ions stimulated by thermal energy as long as the applied electric field is small enough. Ionic conductivity is defined as ionic transport from one site to another site through a defect under the influence of an external electric field. Some of the ion transport models with theories are briefly discussed below [2-5].

The basic equation of ionic conductivity of ion-conducting material can be simply represented by the following equation [6].

$$\sigma = \sum_i q_i n_i \mu_i \tag{2.1}$$

where σ is the ionic conductivity i.e. charge transport across a unit cross-sectional area per second per unit electric field applied. The conductivity is proportional to the (i) amount of charge carriers n_i (ii) mobility of charge carriers μ_i. All the above quantities (right-hand side of the equation) depends on the materials environments [7]. The focus on the study of the

ion transport mechanism in polymer electrolytes made by workers since the discovery of ionic conductivity in alkali metal salt complexes of polyethylene oxide (PEO) by Fenton et al. in 1973 [8]. It has been revealed that the movement of ions takes place by the local motion of the polymer chain segment above the glass transition temperature (T_g). Above T_g, the polymer segment motion is a liquid-like motion that causes the local environment in the polymer electrolyte to change with time and affect the ion transport in the polymer electrolyte.

2.2 Theoretical models for Temperature Dependence of Ionic Conductivity

The temperature dependence of ionic conductivity can be understood using a number of empirical relations such as the Arrhenius equation, Vogel-Tamman-Fulcher (VTF) equation, Williams-Landel-Ferry (WLF) equation, etc. Generally, the crystalline phase in polymer electrolytes exhibits Arrhenius conductivity while the amorphous phase of polymer electrolyte where the liquid-like motion of ions occurs exhibits conductivity given by VTF [3,9]. If the temperature of the polymer electrolyte is below the melting temperature (T_m), the crystalline phase is dominated and conductivity is given by Arrhenius behavior. If the temperature is increased beyond a certain temperature (T_c), the amorphous phase is large enough to create a continuous connection/ path between the amorphous cube in the electrolyte. At this point, the conductivity behavior changes from Arrhenius to VTF. This particular temperature T_c is known as a critical temperature or a percolation temperature.

2.2.1 Arrhenius Theory / Arrhenius Model For Ion Transport

This theory was developed by Swedish Chemist, S. Arrhenius for liquid electrolytes in 1889 [10]. Later it was applied for solid electrolytes. This theory gives the linear relationship for log σ versus 1000 /T. In solid, ion hops from one vacant site to another when the energy of the ion is greater than barrier energy, i.e. activation energy. When an electric field is applied, the ions start hopping along the direction of the field which gives rise to an ionic current density $\vec{J}$ given by

$$\vec{J} = \frac{na^2e^2\nu\vec{E}}{KT} = \sigma\vec{E} \qquad (2.2)$$

where *K* is the Boltzmann constant, n is the number of defects per unit volume which is proportional to the exp (−*G*/2*KT*), where *G* is the Gibbs free energy to create defects in solid electrolytes, *e* is a charge of the ion, *a* is the interionic distance and σ is the ionic conductivity, *v* is the jump frequency i.e., probability of jump from one site to another in the absence of electric field and is given by,

$$\nu = \nu_0 \exp\left(\frac{-\Delta G}{KT}\right) \tag{2.3}$$

where ν_0 is jump frequency and $\Delta G = \Delta H - T\Delta S$, the energy of ion migration, where ΔH and ΔS are the enthalpy and entropy of diffusion respectively. ΔG is the difference between the free energy of the ion at the normal lattice site and that at the top of the energy barrier.

Finally, the ionic conductivity (σ) can be given as:

$$\sigma = \sigma_0 \exp\left(\frac{-E_a}{K_B T}\right) \tag{2.4}$$

where σ_0 is the pre-exponential factor and E_a is the activation energy and K_B is Boltzmann constant.

2.2.2 VTF Theory / Vogel – Tammann – Fulcher Theory

In the VTF model, it is assumed that the ions are transported by some random motion of polymer chains, providing free volume into which the ion can diffuse under the influence of an electric field. The temperature dependence of ionic conductivity can be represented by VTF when the plot of log σ versus 1000 /T is non-linear which is characteristics of ionic motion is coupled with polymer segmental motion of host matrix [11-13]. The VTF equation was first developed to describe the viscosity of supercooled liquids [12].

The VTF relation is given by:

$$\sigma = AT^{-1/2} \exp\left(\frac{-E_a}{K_B(T - T_0)}\right) \tag{2.5}$$

where *A* is the pre-exponential factor, T_0 is the reference temperature associated with glass transition temperature, K_B is Boltzmann constant and E_a is the activation energy.

2.2.3 WLF (Williams – Landel – Ferry) Theory

The WLF equation is an extension of the VTF relation to characterizing the relaxation process in an amorphous system [14]. This equation is given as [15]:

$$\log a_T = \log \frac{\sigma_T}{\sigma_{T_g}} = \frac{C_1(T - T_g)}{C_2 + (T - T_g)} \tag{2.6}$$

where $\sigma(T)$ is ionic conductivity at T and $\sigma\ (T_g)$ is ionic conductivity at T_g, a_T is the mechanical shift factor which represents the fluidity or inverse relaxation time or relaxation rate, and C_1 and C_2 are constant. This formula is usually used to show the temperature-dependent relaxation time in the polymeric material. The temperature-dependent ionic conductivity in amorphous material is the result of the local motion of a chain of polymer within the material. According to the WLF equation, when T_g decrease, the ionic conductivity increases. It is found that the ionic conductivity occurs only in the amorphous polymer at a temperature above T_g.

2.3 Theoretical Models for DC Conductivity

Various theoretical models have been proposed to explain the ion conduction mechanism in disordered materials. Models, which are applicable to polymer electrolytes systems are discussed below:

2.3.1 Free Volume Model

Cohen and Turnbull [16-19] had proposed this model to explain the ion conduction mechanism in polymer electrolytes known as the "Free Volume Model". He considered that the matrix molecules are hard-sphere, so ions are caged in the free volume to diffuse only due to the relaxation of polymer matrix molecules. These voids or free volumes are larger enough to allow the diffusion. The equation for the diffusion of molecules in the system can be expressed as:

$$D = gau \exp\left[\frac{-\gamma V^*}{\alpha \bar{v}_m (T - T_0)}\right] \tag{2.7}$$

where 'g' is a geometric factor, 'a' is molecular diameter, V^* is critical volume, u is thermal velocity, γ is a Lagrange's parameter, α is the thermal expansivity, $\bar{v}_m$ is the mean molecular volume over the temperature range (T-T_0) which arises due to the redistribution of free volume within this liquid. According to this model, in a pure polymer, as the temperature increases, the local empty space (free volume) is created due to the finite expansion of polymer chains. Thus, ions attached to the polymer chain segment can move through this free volume.

Statistical calculation predicts an increase of free volume with temperature follows the equation given below:

$$V_f = V_g[0.025 + \alpha(T - T_g)] \tag{2.8}$$

where V_g is the critical volume per mole at T_g, which is considered as the temperature at which the free volume eventually vanishes, α is the thermal expansivity and T represents the temperature during the experiment.

2.3.2 Configurational Entropy Model

Another group of theories based on the configuration entropy model was proposed by Adam and Gibbs[20] to explain the ion transport in polymer electrolytes [21]. In the case of polymer electrolytes, the conduction process is combined with the effect of ion size, polarizability, ion-pairing, ion-concentration chain length, etc. Free volume theory does not consider all these factors. Hence, Gibbs and Adam modified the free volume theory by considering the entropy changes in the process and named it the "Configurational Entropy Model". According to this model, the mass transport mechanism is assumed to be a group cooperative rearrangement of the chain rather than a redistribution of free volume in the polymer. The average probability of rearrangement of the polymer chain can be expressed as

$$W = A\exp\left(\frac{-\Delta\mu S_c^*}{KTS_c}\right) \tag{2.9}$$

where S_C^* is the minimum configurational entropy required for rearrangement. S_C is the configurational entropy at temperature T and $\Delta\mu$ is the free energy barrier per mole which opposes the rearrangement. Shriver et al.[22] applied the configurational entropy model to polymer electrolyte [23,24].

2.3.3 Static Bond Percolation Model

The static bond percolation (SBP) Model [5] was proposed to describe to explain the microscopic ion transport mechanism in the electrolyte system with a rigid framework. Various properties of polymer electrolytes can be explained by this model. Based on the concept of this model, the ion motion for any fixed polymer configuration is described by a percolation (hopping) process by choosing the rate of hopping between any two sites as finite or zero which depends upon whether these sites are mutually accessible (open bond/

available) or not (close bond/unavailable). The model involves ion hopping between sites on a lattice with the ions obeying a hopping type equation

$$P_i = \sum_j P_j W_{ji} - P_i W_{ij} \tag{2.10}$$

where P_i is the probability of finding a mobile ion at site i, W_{ij} is the probability per unit time that an ion will hop from site j to site i, and vice-versa and is equal to zero except between neighboring sites.

It is then assumed that W_{ij} may take two values,

$W_{ij} = 0$, probability 1- f

$W_{ij} = W$, probability f,

In the standard percolation model, the jumps are either permitted or not permitted, where f denotes the fraction of bonds (the link between localized hopping sites) that are open/ available, and $1 - f$ represents the fraction of bonds that are occupied or unavailable. Thus, this model involves the motion of charge carriers in a certain lattice whose bonds are randomly available with certain availability (f) (Figure 2.1). Using the static bond percolation model, it has been successfully explained that why the crystalline phase has no conductivity and the amorphous phase is responsible for ionic conduction in the polymer electrolyte system [25].

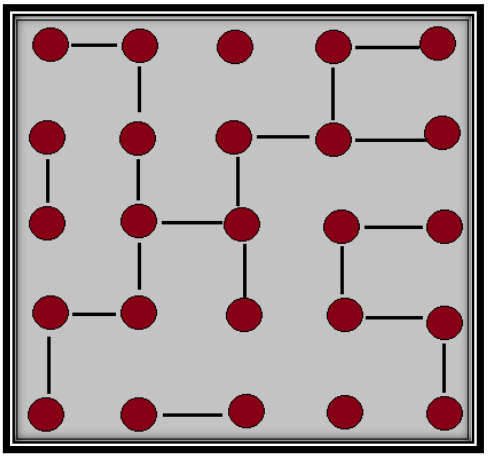

Figure 2.1 A percolation pattern, with available fraction of bond which is a pathway for the motion of ions between available sites.

Whereas in the case of the gel polymer electrolyte, a large amount of low molecular weight plasticizers is added. This forms a wide network for the conduction of mobile ions while polymer matrix provides structural support. This provides a percolative path for the conduction of ions and conductivity increases. Aziz et al.[26] elaborated the conduction

mechanism in gel polymer electrolyte and shown the percolative path for the transportation of ions through amorphous and solvent swollen amorphous polymer matrix as shown in Figure 2.2.

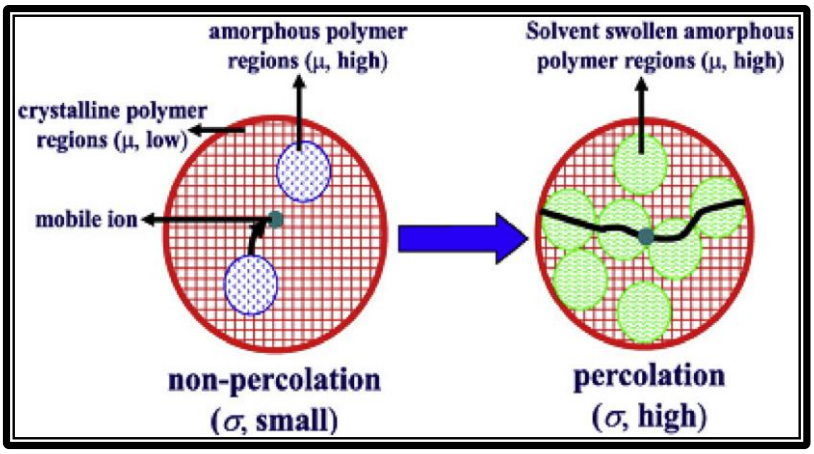

Figure 2.2 Schematic diagram of non-percolation and percolation path for ion transportation in the amorphous and solvent swollen polymer.

2.3.4 Dynamic Bond Percolation Model (DBP)

Druger, Nitzan, and Ratner [27-31] had proposed the dynamic bond percolation which is an extension of the static bond percolation model (SBP). In this model, the material is considered to be made up of a dynamic framework instead of a rigid framework. The dynamic framework means where the open and closed bond positions are continuously changing. In other words, the structure is not statically but dynamically disordered. Motion of ions in polymer electrolytes is strongly depended on segmental motion of polymer chain and conductivity is observed at temperature above glass transition temperature (T_g). This is the microscopic model which takes into account in polymer electrolytes where ionic motion is result of combination of the ionic transition motion/ hopping of charge carrier and dynamic polymer segmental motion when $T > T_g$. The lattice sites in polymer electrolytes are no longer static but rearrangement process occurs which re-assign the open and closed bonds when $T > T_g$. Ion transport mechanism involves a comparison of a structural relaxation time, τ_s and a conductivity relaxation time τ_σ.

2.3.5 Space Charge Model

In some 2-phase composite electrolyte systems, the enhancement of the ionic conductivity (σ) can be explain based on this space charge model. In this model, it is suggested that the

layer is present near the boundaries of ceramic fillers in the composite electrolytes system known as the space charge layer. These layers overlap each other with increasing the concentration of filler which provides conducting pathways. Maier et al. [32] suggested the system called 'Soggy Sand' electrolytes which were used for the viscous grain liquid electrolytes having a high concentration of ceramic filler particles. According to him, ionic conductivity increases with increasing the ceramic filler content due to interfacial interaction occurring on the ceramic grain boundaries, which leads to the absorption of anions resulting in a break of ion-pair and generate mobile counter ion. As a result, an increase in the charge carriers (cations) takes place around nanofiller in the region of the space charge layer as shown in Figure 2.3.

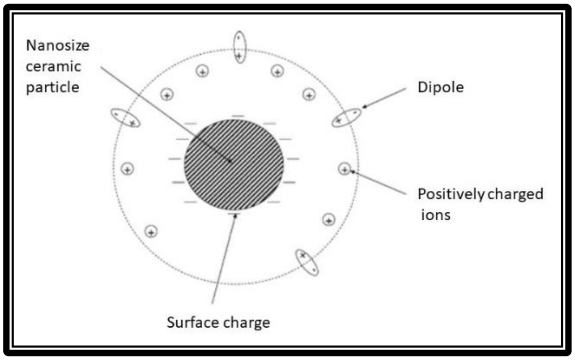

Figure 2.3 Space charge layer around nano-sized particles [33]

2.3.6 Amorphous Phase Model

For the composite polymer electrolyte system, the amorphous phase model explains the increase in ionic conductivity due to its increased amorphous nature [34]. It is observed by the different workers that the reduction in crystalline nature is due to the dispersion of ceramic filler as compared to the undispersed system [35]. Based on this result, the Amorphous phase model was developed [36]. For example, in a PEO based crystalline system, when filler particles (e.g. α - Al_2O_3) are dispersed, it acts as nucleation centers and probably attached to the segment of PEO. Since there is a large number of nucleation centers, the crystallization process becomes faster as a result higher level of disordered structure is created.

The schematic diagram of the amorphous phase model is shown in Figure 2.4 which shows three phases: an isolated filler grain (2), surrounded by highly conductive interfacial layer coating (1), and immersed in the bulk polymer electrolyte matrix (3).

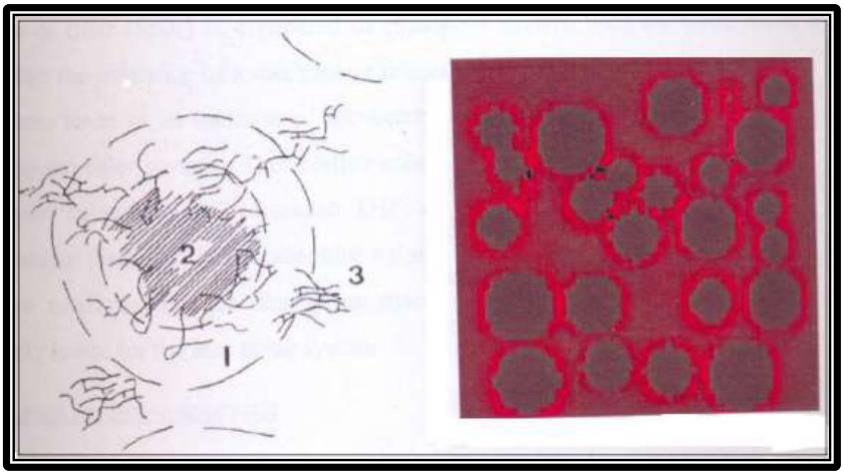

Figure 2.4 Schematic diagram of the morphology of composite polyether non-conductive filler electrolytes [25]

2.3.7 Effective Medium Theory

Effective Medium Theory was proposed by C. W. Nan & Smith [37] to explain the effect of insulating fillers and consequent enhancement in the conductivity in the CPE system [38]. The reason behind the enhancement in conductivity is attributed to high defect concentration on the surface of filler grains due to the formation of 'space-charge' layers. Like the amorphous phase model, the effective medium theory also assumed the presence of three phases in composite polymer electrolytes as shown in Figure 2.5.

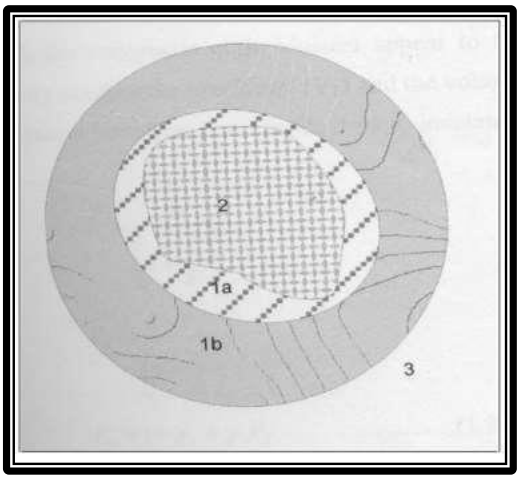

Figure 2.5 A schematic representation of a polymer matrix with a single nanofiller grain dispersion [33]

Phase (1-a) represents part of the amorphous shell formed on the grain surface. Phase (1-b) represents a highly conductive (due to amorphization) interface layer coating on the surface of the grain. Phase (2) is the dispersed insulating grain in the matrix of the ion-conducting

polymer. In phase (3), the composite grain units are dispersed all over the polymer matrix, and a highly conducting interface layer covering the surface of grains overlaps with each other results in the formation of high conductive pathways.

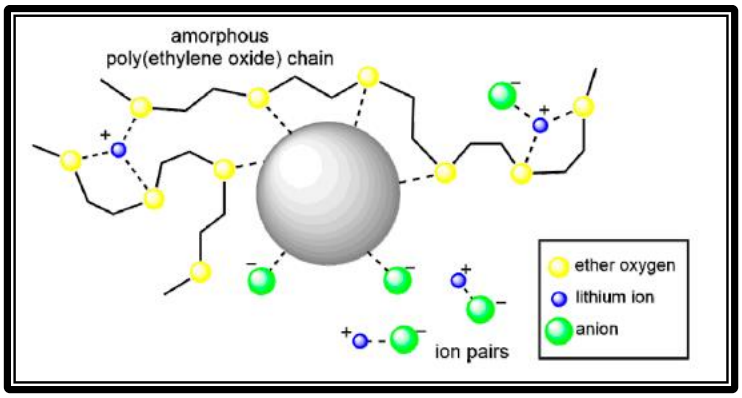

Figure 2.6 Schematic of Lewis acid-base interactions between a PEO–$LiClO_4$ electrolyte host and a nanoparticle guest [39].

2.4 Theories of Explaining Plasticization

The addition of plasticizers in the polymer electrolyte is explained here. Plasticizers are an important additive to improve the properties of the polymer electrolyte system such as a reduction in hardness, viscosity, lowering the glass transition temperature, and effect on the polymer's chain flexibility. Plasticizers are low molecular weight polymers having a polar group in them which interacts with the polar group of the polymer chain cause reduction of crystallinity and enhance the flexibility of the polymer chain [40]. However excess use of plasticizer reduces the mechanical stability and more reactive toward electrode results in the reduction of the lifetime of devices. The lubricity theory, the gel theory, or the viscosity theory were developed during the 1940s. Later free volume theory was developed.

2.4.1 The Lubricity Theory

According to Kilpatrick [41], Clark [42], Houwink [42], the addition of plasticizers reduces the intermolecular forces between the polymer molecules. By doing so, polymer chains are allowed to move freely throughout the material (Figure 2.7). According to this theory, one segment of the plasticizers strongly attracts polymer molecules whereas the other is free. The former acts as a solvent while the latter act as a lubricant.

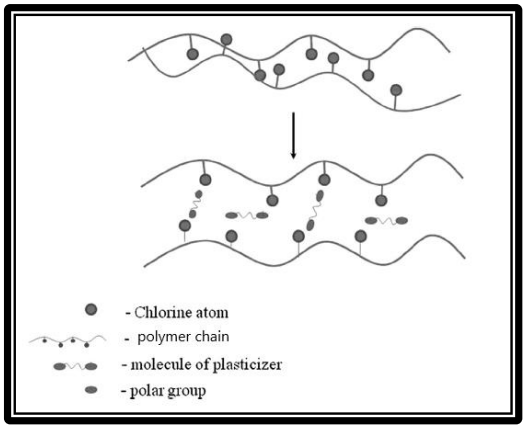

Figure 2.7 Lubricity theory explaining plasticizers-polymer response [40]

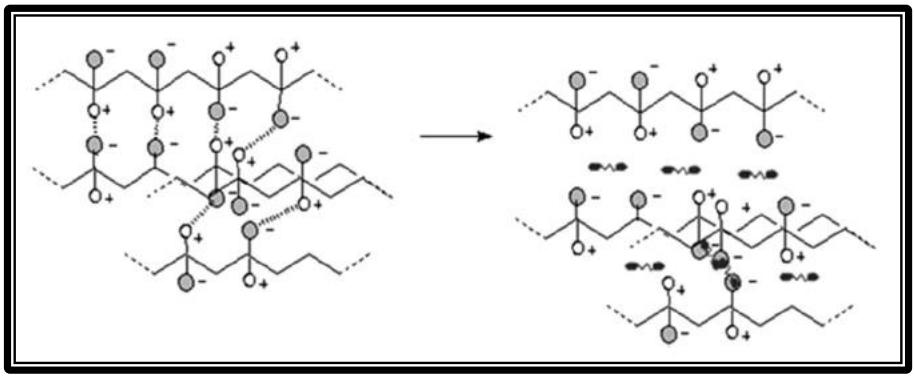

Figure 2.8 Plasticizer polymer action based on gel theory [40]

2.4.2 Gel Theory

The other theory of plasticization namely gel theory was developed by Aiken and others [43]. This theory is an extension of lubricant theory, where plasticizers reduce the loose attachment between the polymer chain which have formed the 3-dimensional honeycomb or gel structure [44]. The loose attachment between the polymer chains may be due to Van der Waals forces or crystalline structure. By separating them upon the addition of plasticizers, the free movement of the polymer chains is feasible (Figure 2.8).

2.4.3 The Free-Volume Theory

The free volume theory discusses the quantitative assessment of the plasticization process in the polymer matrix. Many authors have contributed to this theory but originally, it was postulated by Fox and Flory [45].

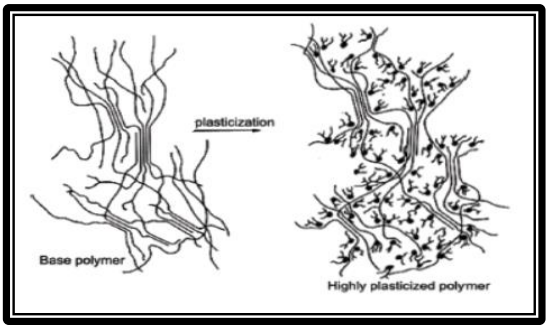

Figure 2.9 Schematic representation of increased free volume upon addition plasticizers [46]

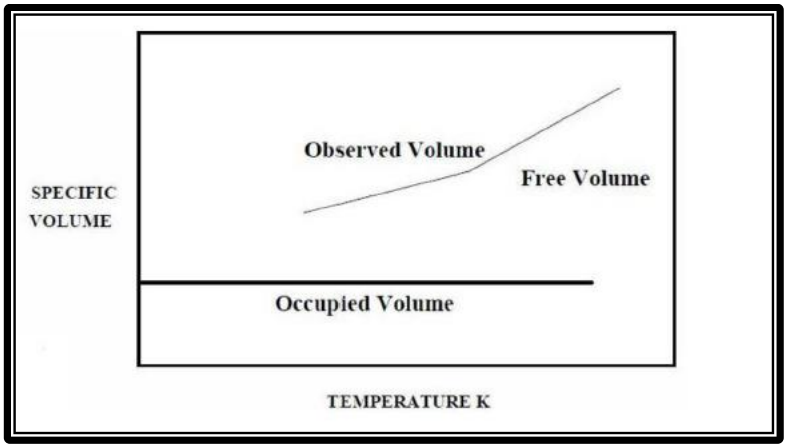

Figure 2.10 Specific free volume -temperature curve

The free volume means available free space where the degree of freedom of the polymer chain is more. A glassy state of the polymer, where little free rooms are available for the movement of the polymer chain makes the material stiff. The change in the state of the polymer from hard to rubbery depends on the glass transition temperature of polymers. As plasticizers are incorporated in it and its temperature is above the glass transition temperature, this leads to the separation of the polymer chain and more free volume within the polymer matrix is available (Figure 2.9). The free volume theory gives clarification on the reduction of glass transition temperature with plasticizers. The specific volume of the polymers is also found to increase after the glass transition temperature of the polymer (Figure 2.10).

2.5 Impedance Spectroscopy and Various Conductivity Formalisms.

2.5.1 Complex Impedance Spectroscopy (CIS)

AC impedance spectroscopy or complex impedance spectroscopy is a powerful non-destructive technique for the characterization of electrical properties to evaluate the electrochemical behavior of the electrode as well as electrolyte material. The fundamental approach of complex impedance spectroscopy to study the electrical impedance response of the solid-state ionic material under the application of small amplitude sinusoidal voltage (ac signal) of different frequencies ranging from mHz to MHz (10 Hz to 10^6 Hz). Impedance analysis of ion-conducting material is useful to identify dynamical responses such as total (bulk) conductivity, ion transport, dielectric properties of materials, grain-boundary conduction (in case of crystalline compositions), electrode-electrolyte interface processes and relaxation processes, etc. The impedance spectroscopy measures the cell impedance over a wide range of temperatures and frequencies and analyzing them in a complex impedance plane [47,48].

The measurement of electrical conductivity of ion-conducting materials is not as simple as that of electronic materials. In the case of the electronic conductor, application of D.C. voltage across the sample results in the generation of current, whereas application of D.C. voltage across ionic conductor leads to fast interfacial polarization, which results in an increase in the resistance as a function of time [49,50]. To avoid or in order to overcome this difficulty, the A.C. method has been adopted. Both D.C. and A.C. methods are described in detail given below:

(a) Direct Current (D.C.) Method

In this method, a constant potential (voltage) or current is applied across the sample, which is generally sandwiched between two non-blocking (reversible electrodes), and the resulting current or voltage is measured. The conductivity can be calculated by the following relation

$$\vec{J} = \sigma \vec{E} \ \& \ \sigma = \frac{I}{V} \cdot \frac{l}{A} \text{ [from ohm's law]} \tag{2.11}$$

where V is voltage, I is current, l is the thickness of the sample, A is cross-sectional area. Two common methods are used namely, first 'Two probes', and second one is 'Four probes' techniques. In the two probes method, a known value of D.C. voltage is applied across the sample and the resulting current is measured to know D.C. resistance and hence conductivity can be estimated of a sample. In the four-probe method, a known D.C. current is applied between two outer electrodes, and the resulting potential is measured between two inner

electrodes. Conductivity can be measured by knowing the area of electrodes and the distance between them.

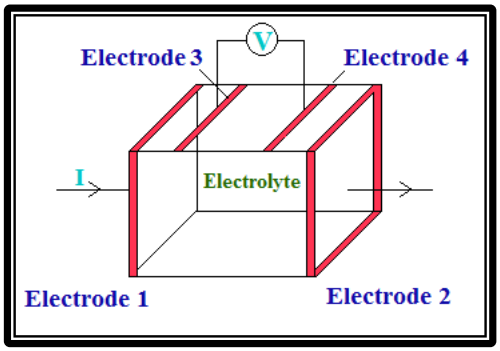

Figure 2.11 Set up for four probes method [50]

This method is not adequate and correct to measure the conductivity of ionic conductor (polymer electrolytes) which is limited due to the following factors:

(i) Electrode – electrolyte contact resistance.

(ii) Grain boundary effect.

(iii) Electrode – electrolyte interfacial polarization.

(iv) Difficulty in getting proper reversible electrodes for both the cations and anions.

Hence, the A.C. method is preferable to measure bulk conductivity in ionic conducting materials.

(b) Alternating Current (A.C.) Method (Electrochemical Impedance Spectroscopy, EIS)

In the A.C. method or impedance spectroscopy techniques, a small amplitude of the sinusoidal electrical signal (A.C. signal) is applied to a sample, which is sandwiched between either blocking or non-blocking electrodes, and the corresponding current is measured to determine impedance as a function of frequency and analyzing them in the complex impedance plane. The complex impedance plane (Z^*) which involves real and imaginary part of the complex electrical quantities, also known as the Nyquist Plot which gives information about bulk conductivity and transport properties. The electrolyte sample consists of resistance and capacitance which is frequency-dependent, hence, impedance $Z = R + jX_c$ is frequency-dependent.

The applied A.C. voltage and the resulting current across a cell have the form,

$$V = V_{max} \sin(\omega t)$$

$$I = I_{max} \sin(\omega t + \phi)$$

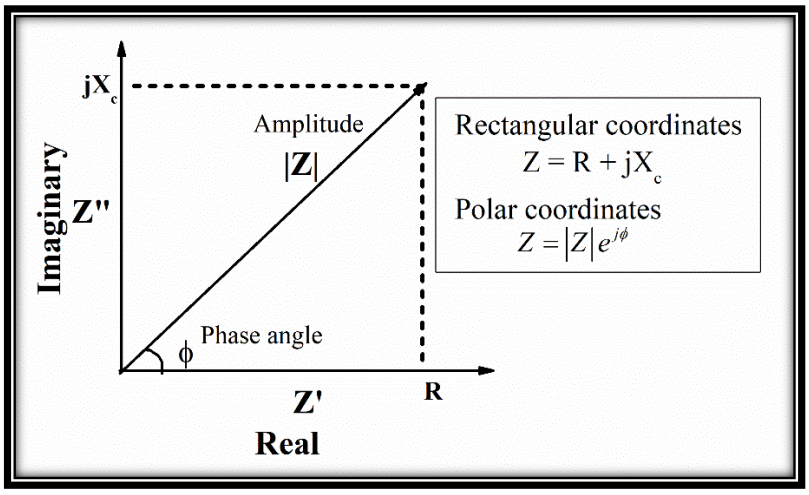

Figure 2.12 AC complex impedance plot in the complex plane

where ϕ is the phase angle corresponds to phase difference between the applied voltage and current and ω = 2πf, f is the frequency of measurement. The magnitude of the impedance is given by | z | = $\frac{V_{max}}{I_{max}}$. The typical AC complex impedance plot in the complex impedance plane is depicted in Figure 2.12. The impedance is composed of frequency-independent resistive term R and a capacitive term $1/j\omega C$, where, $j = \sqrt{-1}$. The complex impedance Z^* is expressed in terms of real and imaginary terms by the following equation

$$Z^* = Z'(\omega) - jZ''(\omega) \tag{2.12}$$

where Z′(ω) and Z′′(ω) are the real and imaginary part of the impedance.

$$Z'(\omega) = |Z|\cos\theta \tag{2.13}$$

$$Z''(\omega) = |Z|\sin\theta \tag{2.14}$$

The complex impedance Z^* has both magnitude $|Z|$ and phase angle ϕ and can be expressed in both polar as well as cartesian forms.

In polar form, complex impedance $Z(\omega)$ may be written as

$$Z^*(\omega) = |Z|\exp(-j\phi) \tag{2.15}$$

where ϕ is expressed as $\phi = \tan^{-1}\frac{Z''}{Z'}$. Magnitude $|Z| = \sqrt{Z'^2 + Z''^2}$ and $\exp(-j\phi) = \cos\phi - j\sin\phi$.

The obtained complex impedance from EIS can be compared or fitted with an equivalent circuit model comprising of resistor, capacitor, and an inductor or their series and parallel

combination which represent charge migration as well as polarization phenomena within the cell. Impedance plots for a pure resistance (R), capacitance (C), and their series as well as a parallel combination are shown in Figure 2.13. The equivalent circuit depends on the types of electrodes (reversible or irreversible) and electrolytes with single mobile ion species or double mobile ion species. The impedance plot of a pure resistor is a point on a real axis and a capacitor is a straight-line coinciding line parallel to Z''- axis at $Z' = R$ is expected. Disordered electrolyte systems can be analyzed in terms of capacitive and resistive behavior. The impedance of a parallel RC combination is expressed as:

$$\frac{1}{Z^*} = \frac{1}{R} + \frac{1}{1/(i\omega C)} \tag{2.16}$$

$$Z^* = \frac{R}{1 + i\omega RC} \tag{2.17}$$

$$Z^* = \frac{R}{1+\omega^2 R^2 C^2} - i\frac{\omega R^2 C}{1+\omega^2 R^2 C^2} \tag{2.18}$$

where $Z' = \frac{R}{1+\omega^2 R^2 C^2}$ and $Z'' = -\frac{\omega R^2 C}{1+\omega^2 R^2 C^2}$.

When ω = 0, $Z' = R$ and $Z'' = 0$ when $\omega = \infty$, $Z' = 0$ and $Z'' = 0$. Between these extreme values it can be seen that Z' and Z'' comply with the following equation:

$$\frac{R^2}{4} = \left(Z' - \frac{R}{2}\right)^2 + Z''^2 \tag{2.19}$$

$$\left(\frac{R}{2}\right)^2 = \left(Z' - \frac{R}{2}\right)^2 + Z''^2 \tag{2.20}$$

This is an equation of a circle with a radius $\frac{R}{2}$ and center at $\left(\frac{R}{2}, 0\right)$ as shown in Figure 2.13 (d). Thus a plot of Z'' vs. Z' will result in a semicircle of radius $\frac{R}{2}$ which represents the response of a resistor *R* in parallel with capacitor *C* which will be a perfect semicircle intersecting the real axis at (*R*, 0). This plot is known as the 'Nyquist plot' or 'complex impedance plot', with the time constant or relaxation time $\tau = RC = 1/\omega_{max.}$ When an ideal electrolyte sandwiched between two blocking electrodes, the response of the Nyquist plot consist semicircle (at high frequency) whose center lies on the real axis and the system can be regarded as a combination of a resistor (R) and a capacitor (C) connected in parallel

followed by spikes (Figure 2.14 a). The spikes at low frequency are observed in the typical Nyquist plot due to the blocking electrode which does not allow the ions to move in the outer circuit, merge or react with electrodes. At the low frequency of applied ac field, ions get accumulated at the surface of the electrode has the tendency to attract opposite charge ultimately form a double layer of charges at the electrode-electrolyte interface often referred to as "double-layer capacitance (C_{dl})". But the impedance spectra for the real electrolyte system is usually complicated. The Nyquist spectra consist of depressed or distorted semicircle and slanted or tilted spikes (Figure 2.14 b). A depressed semicircle represents the bulk properties of electrolyte whereas a spike represents electrochemical double-layer capacitance. For this distorted semicircle, the center of it lies below the real axis. For the polymer electrolyte system, this type of behavior has been observed by many researchers. Such deviation of impedance from the expected ideal behavior may arise due to properties of an electrolyte having the presence of inhomogeneities, distributed microscopic properties, non-uniform diffusion, non-ideal capacitive behavior (leaky capacitor), etc. and inclined spike at low frequency may come into the picture due to unevenness or roughness of the electrode/electrolyte interfaces, diffusion of species in the electrode/electrolyte interfaces. This deviation from the ideal behavior introduces a new element in the equivalent circuit termed as "Constant Phase Element (CPE)" instead of a pure capacitor (C) element. A wide range of reported materials has shown depressed semicircle indicating distributed element or distributed microscopic materials properties [51,52].

In the case of polycrystalline materials, the electrolytes are to be considered as made up of crystalline region separated by grain boundary as shown in Figure 2.15(a). When the polycrystalline sample is sandwiched between the electrodes, the arrangement of the cell is regarded to be composed of the crystalline region (grain) + grain boundary + electrode/electrolyte interface. The conduction process occurs inside the grain (bulk conduction) along with grain boundaries (intergrain conduction). The two regions e.g. grains and grain boundaries can be considered to have two parallel R- CPE elements in series which followed by the CPE element arise as a result of an effective double-layer capacitance due to the electrode/electrolyte interfaces. Impedance plot for the same with the equivalent circuit is shown in Figure 2.15(b). First semicircle due to the presence of grain in polycrystalline material whereas the second semicircle represents the grain boundary effect. Conduction occurs inside the grain (intragrain or bulk conduction) and along grain

boundaries (intergrain conduction). It is assumed to be a faster movement of ions through the grain under the application of an AC electrical field.

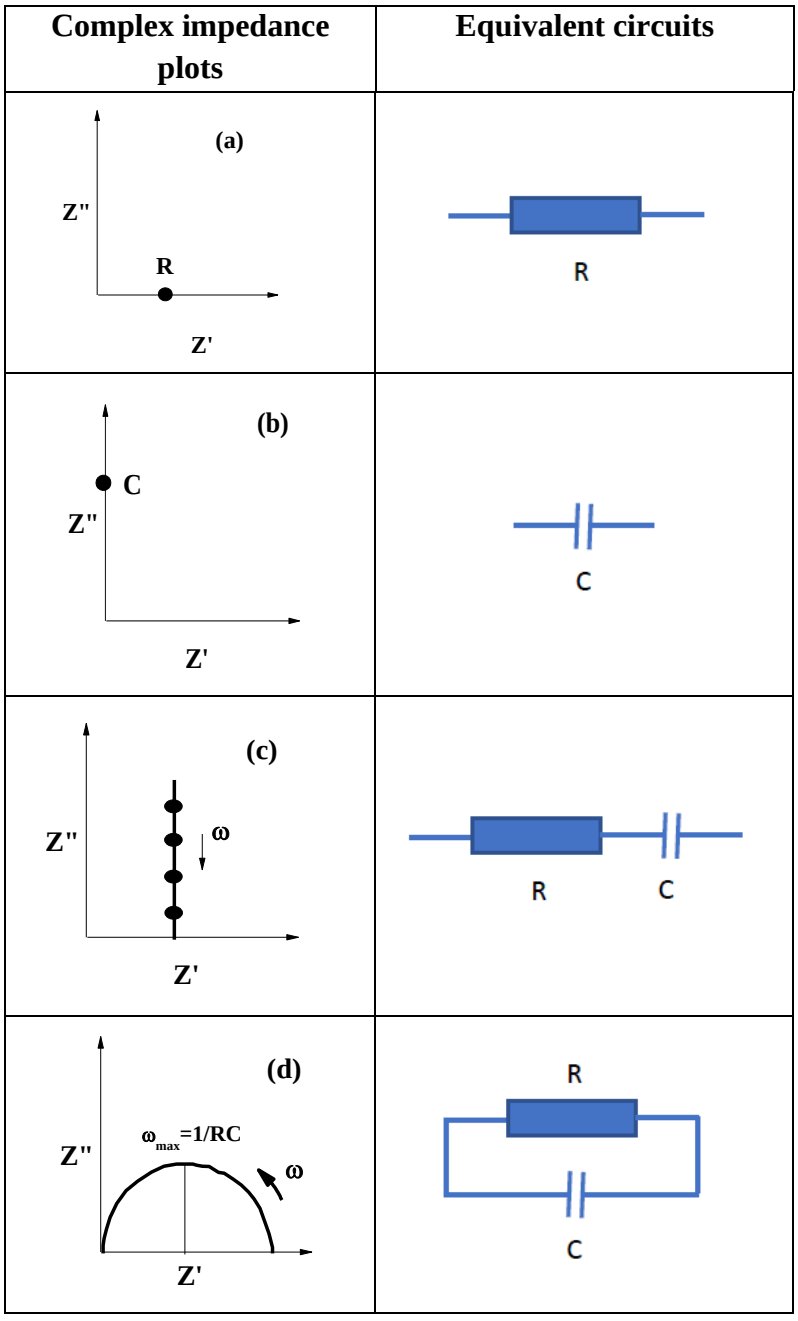

Figure 2.13 Complex impedance plots and equivalent circuits

The study of the Nyquist plot provides information regarding ion transport through polymer electrolyte. However, the impedance plot does not show direct frequency associated with it

so it is difficult to find the frequency-dependent parameter such as relaxation occurring inside the materials. In such cases, to inspect relaxation and dielectric behavior, the data are plotted using other functions associated with the impedance such as permittivity, electrical modulus, admittance. The relationship of all these functions with the impedance are given in Table 2.1. In the present work, impedance spectroscopy measurement has been carried out to determine the bulk conductivity of the polymer electrolytes as a function of composition and temperatures.

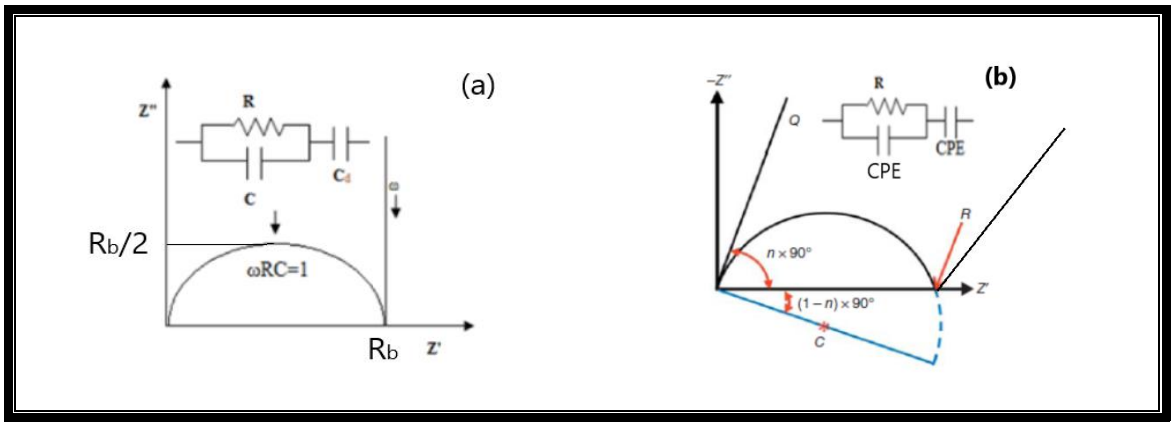

Figure 2.14 Complex impedance plot of (a) ideal system (b) real system.

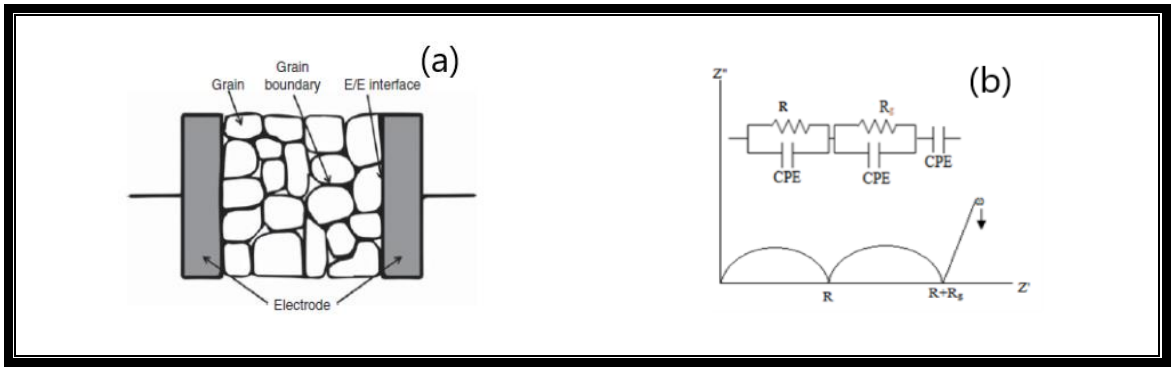

Figure 2.15 (a) A polycrystalline sample sandwiched between electrode (b) Impedance plot of polycrystalline system.

2.5.2 Dielectric spectroscopy Techniques

Generally, active dielectric material possesses a microscopic mechanism of dielectric polarization under the time-varying electric field. Thus, this type of material is suitable for energy storage applications. The process of relative shifting of the negative and positive charges within the dielectric material under the application of an external electric field is known as dielectric polarisation. We can write the relation between polarisation P and electric field E as:

$$\vec{P} = \varepsilon_0 \chi \vec{E} \tag{2.21}$$

where ε_0 is the permittivity of free space, 8.854×10^{-12} F/m and χ is susceptibility.

Different mechanism of polarizations are involved in this process namely electronic or atomic polarization, ionic polarisation, orientation or dipolar polarization, space-charge or interfacial polarization [53]. Figure 2.16 shows the different polarisation mechanisms in an insulating material.

Electronic or atomic polarization: A slight displacement of the electron of an atom with respect to the positive nucleus under the influence of an electric field is called electronic polarization. This type of polarization usually occurs at a higher frequency i.e. optical frequency.

Ionic polarisation: The shifting of positive ion in the direction of the applied field and negative ion in the opposite direction of the applied field. This type of polarization is known as ionic polarisation. This type of polarisation is observed in ionic solid.

Orientation or dipolar polarization: The alignment of permanent dipoles under the application of an applied field creating a net polarization, is called dipolar polarization. Dipolar polarization occurs in the material which possesses permanent dipoles. This polarisation occurs in the microwave frequency region.

Space-charge or interfacial polarisation: The accumulation of positive and negative charges at negative and positive electrodes gives rise to polarization is called interfacial polarization. This kind of polarization occurs in dielectric material at a lower frequency where ions are capable to migrate over some distance through the bulk region of the material.

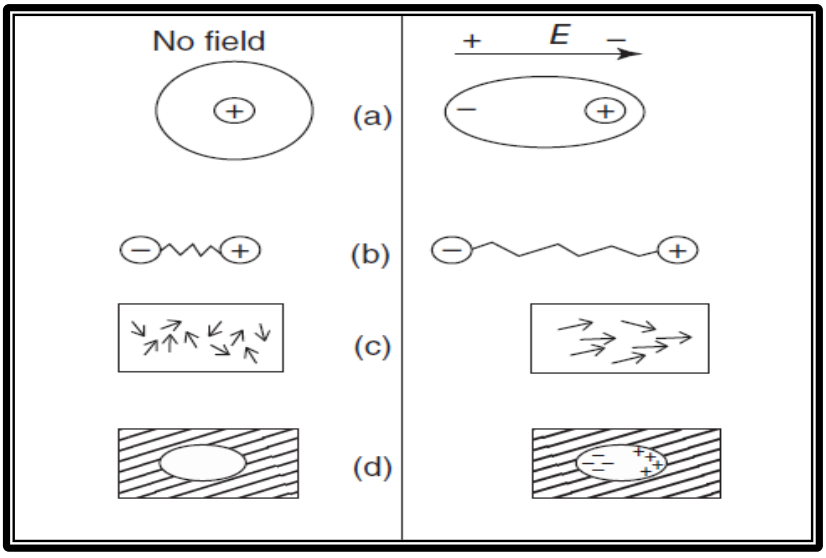

Figure 2.16 Schematic representation of polarisation (a) Electronic or atomic polarization (b) Ionic polarisation (c) Orientation or dipolar polarization (d) Space-charge or interfacial polarisation [54]

Effect of frequency on polarization

The dipoles of dielectric material align in the direction of the applied field when it is placed in an alternating electric field. The orientation of dipole requires a finite time to polarise. The displacement of charges occurs. The displacement of charges is linearly proportional to the applied field ($D \propto E \Rightarrow D = \varepsilon E$) and the proportionality constant is called the permittivity (ε). When AC field is applied to dielectric material the permittivity is represented by a complex number or complex dielectric (ε^*) given as [55]

$$\varepsilon^* = \varepsilon'(\omega) - i\varepsilon''(\omega) \tag{2.22}$$

where ε′ is real and ε″ is the imaginary part of complex permittivity, respectively. Here ε′ also known as a dielectric constant which measures the charge storage in the material and ε″ is dielectric loss and it measures the energy dissipation by the material to an external field.

The dipoles are able to reorient themselves along in the field direction when the frequency of dipole matches with the frequency of the AC field is called relaxation frequency. At this frequency, the dielectric loss that is energy loss in the form of heat would be maximum. Above the relaxation frequency, dipoles will no longer be able to align with the change in the frequency of the applied field and the polarization becomes "frozen" and no longer contributes towards polarisation. Figure 2.17 shows the different polarisation mechanisms as a function of frequency. At higher frequency i.e., optical frequency, only electronic polarisation occurs and the peak is observed at the frequency ~ 10^{15} Hz due to resonance

effect. The dipolar polarization occurs in the microwave frequency region where dipoles are able to respond with field and loss is maximum at the resonant frequency. The space charge polarisation has a slower response to frequency. The polarisation mechanism gives rise to the dielectric constant and dielectric loss of the material.

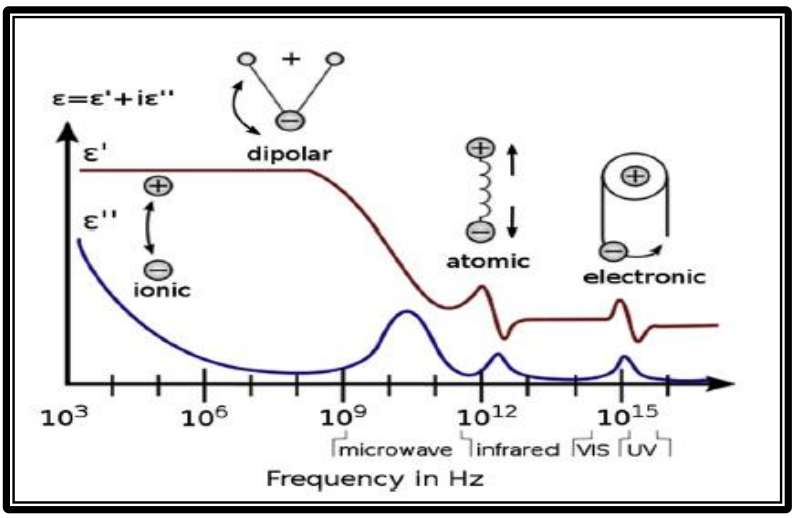

Figure 2.17 Dielectric constant, dielectric loss, and different polarization mechanisms as a function of frequency [56].

As shown in Figure 2.17, the material consists of different types of polarization occurring in electronic, atomic, ionic, dipolar, etc. with different relaxation times in the system within a particular frequency range. This data is represented by using this formalism (Eq. 2.22) to provide the dielectric properties of the materials. Dielectric properties provide information regarding the polarization phenomenon occurring in the materials such as ion polarization, molecular motion, and their dielectric relaxation behavior [57,58]. A frequency-dependent dielectric study was reported by Cole-Cole [59] and thereafter it was adopted to characterize a wide variety of solid materials. Dielectric formalism has been used to investigate dipolar relaxation in solids and liquids where reorientation of permanent dipoles give rise to characteristic frequency-dependent features of the complex permittivity [59].

Dielectric polarization was first proposed by Debye in 1912. It is given below

$$\varepsilon^*(\omega) = \varepsilon_\infty + \frac{\varepsilon_s - \varepsilon_\infty}{1 + i\omega\tau} \tag{2.23}$$

where τ is the relaxation time of the dipoles, ε_s and ε_∞ are the static and high-frequency dielectric parameters. The Eq. 2.23 is known as the Debye equation for the system with a single relaxation time.

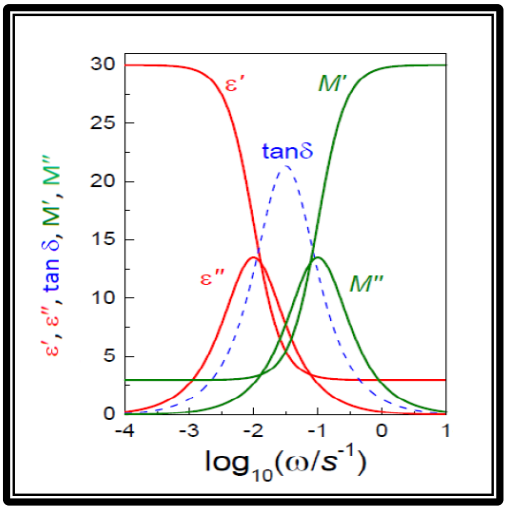

Figure 2.18 Schematic representation of Debye relaxation behavior [53]

In practice, very few materials obey Debye type relaxation having a single relaxation time. In disordered materials, e.g. amorphous materials, polymers or glasses, it is often found that the peak is broader than the Debye peak which can be interpreted as distributions of relaxation times rather than single relaxation time [52,60].

The loss of power in the form of heat under the application of an electric field is known as dielectric losses. In the ideal dielectric, the current leads to the voltage by 90° under application of alternating voltage (Figure 2.19).

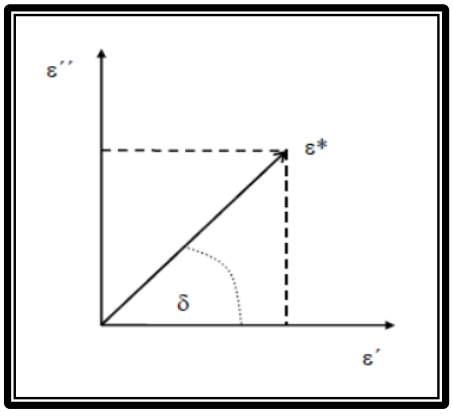

Figure 2.19 Vector diagram of complex dielectric permittivity

From the complex plane,

$$\tan\delta = \frac{\varepsilon''}{\varepsilon'} \qquad (2.24)$$

The above equation referred to as "tangent loss" is the ratio of the imaginary part ε″(energy lost) to real part ε′ (energy stored) of dielectric permittivity. A typical plot of tan δ shows a well-defined characteristic peak as shown in Figure 2.18. The tangent loss is an important parameter to describe the dielectric properties of the polymeric material [55].

2.5.3 Modulus Formalism

The electric modulus was first introduced by McCrum et al. and defined as reciprocal of complex permittivity [61,52].

$$M^*(\omega) = \frac{1}{\varepsilon^*} = j\omega C_0 Z^* = M' + jM'' \tag{2.25}$$

$$M' + jM'' = \frac{\varepsilon'}{\varepsilon'^2 + \varepsilon''^2} + \frac{j\varepsilon''}{\varepsilon'^2 + \varepsilon''^2} \tag{2.26}$$

This formalism was applied by Macedo et al. to analyze the relaxation process in the ionic conductor [62]. Hodge et al., have also stressed the electric modulus for dealing with ion-conducting materials, for the reason it emphasizes on bulk properties of the materials [63]. The main advantage of using Modulus formalism is to eliminate the factitious effect due to two material's interface or contact (Maxwell–Wagner effect). Due to the difference between the relaxation time of charge carriers in these two materials, charges accumulate at the interface of two materials known as Maxwell–Wagner effect [64]. Modulus spectroscopy suppresses the effect of electrode polarization and highlights the bulk conductivity [65]. The complex modulus (M^*) formalism is used to investigate the conductivity relaxation phenomenon [66]. The modulus plot shows typical features as shown in Figure 2.18 where M′(real part of the modulus) exhibits a step-like behavior and imaginary part of modulus M″ exhibits a sharp peak called Debye peak (FWHM = 1.44) with a single relaxation time. This type of behavior is generally observed for the ideal solid electrolyte for which the center of the semicircle (represented by parallel R and C combination) lies on the real axis. But in the real solid electrolyte (e.g. amorphous material, polymers, glasses), a depressed semicircle is observed whose center of the semicircle lies below the real axis (Figure 2.14 (b)). Hence, modulus spectra shows asymmetric and broader than Debye peak with a wider distribution of relaxation time [67].

Furthermore, the electric modulus (M^*) can be expressed as the Fourier transform of a relaxation function $\phi(t)$

$$M^* = M_\infty \left[1 - \int_0^\infty \exp(-\omega t) \left(-\frac{d\phi}{dt} \right) dt \right] \tag{2.27}$$

Further, the broader nature of M'' than Debye peak can be well ascribed by stretch exponential Kohlrausch-Williams-Watt (KWW) function represented by [62]

$$\phi(t) = \phi_0 e^{-(t/\tau)^\beta} \tag{2.28}$$

where $\phi(t)$ function is the time evolution of the electric field within the material, τ is characteristic relaxation time and β ($0 < \beta < 1$) is the stretching exponent. The β can be extracted by knowing full width at half maximum (FWHM) using the following relation

$$\beta = \frac{1.14}{FWHM} \tag{2.29}$$

If the value of $\beta \neq 1$, then it denotes the departure from ideal behavior.

The left side of the M''_{max} (Figure 2.18) determines the long-range motion of charge carriers and contributes to DC conductivity, whereas on the right side of it ($f > f_{max}$), the charge carriers are confined to their potential well and short range of the motion of charge carriers.

The frequency corresponds to a peak in M'' spectrum is called characteristics frequency f_{max}. The conductivity relaxation time can be given by the following relation

$$\omega_{max} \tau = 1 \tag{2.30}$$

Where $\omega_{max} = 2\pi f_{max}$ is angular frequency corresponds to peak maxima and τ is conductivity relaxation time.

2.6 Frequency-Dependent Conductivity

To study the ion conduction mechanism in polymer electrolytes, the application of the AC field plays an important role. Generally, the electrical characterization can be done by application of DC and AC electric fields to the materials. In the case of the application of the DC field to ionic material results in the polarization of material hence it can be applied to only electronic materials, not to ionic or mixed electronic-ionic systems. To resolve this problem, the AC technique is preferable over the DC technique. A large number of studies

has been carried out to investigate the ion conduction mechanism in an ionic conductor by application of AC field [68].

2.6.1 Jonscher's Power Law

The charges in the ionic conductor can migrate under the application of an electric field and it measures the flow of charge carriers. The frequency-dependent ionic conductivity generally follows Jonscher's power law [60].

$$\sigma(\omega) = \sigma_{dc} + A\omega^n \tag{2.31}$$

where $\sigma(\omega)$ is the total ionic conductivity, σ_{dc} is the direct current (DC) ionic conductivity. $A\omega^n$ is a dispersive component of AC ionic conductivity which is power low as a function of frequency, where *A* is pre-exponential factor measure the strength of polarizability and *n* frequency exponent represent the degree of interaction between ions and lattice or its environment.

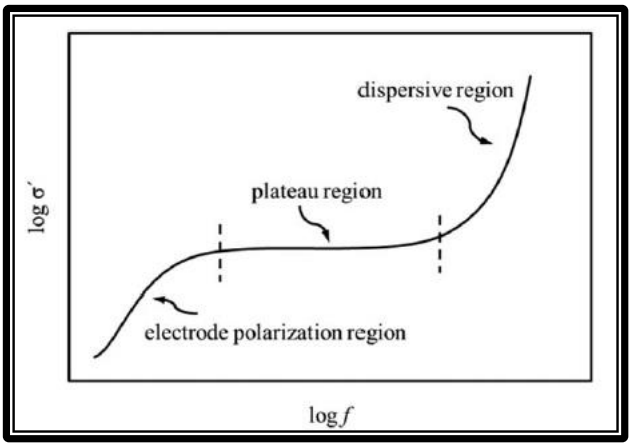

Figure 2.20 Typical AC ionic conductivity plot (log σ′ vs. log f) for ionic conductor [69]

A typical plot of the AC ionic conductivity (log σ′ vs. log f) is shown in Figure 2.20. Generally, the AC conductivity behavior shows three regions (i) low- frequency dispersive region due to an electrode- polarization. (ii) mid-frequency plateau region (iii) high-frequency dispersive region. The low-frequency dispersive region is due to the accumulation of charges at the electrode-electrolyte interface where slow periodic reversal of the electric field is present. The mid-frequency region is the plateau region (almost constant values with the change in frequencies) corresponds to DC conductivity. This is due to the long-range

diffusion of ions from one available site to another. The high-frequency dispersive region follows a power law $\sigma(\omega) \propto \omega^n$. The conductivity increases sharply with an increase in frequency. This power-law behavior has been observed in a wide range of disordered materials, hence called "Universal Power Law" by Jonscher [60,70]. Initially, Jonscher constrained the values of n to be $0 < n < 1$, then it was extended to $n > 1$ with time as it was found to be greater than 1 in many kinds of literature [71-73].

In a time-varying field, the complex quantity can also be displayed in different forms such as complex admittance (Y^*), complex permittivity (ε^*), complex modulus(M^*), loss tangent ($\tan\delta$), etc. To study ion dynamics, various formalisms of impedance spectroscopy is used. All these formalisms are related to complex impedance (Z^*) and are given in Table 2.1.

Table 2.1 Different formalisms of Impedance spectroscopy

Formalism	Equation	
Impedance	$Z^* = Z' - iZ''$	(2.32)
	$Z' = \lvert Z\rvert\cos\phi$ $Z'' = \lvert Z\rvert\sin\phi$	(2.33)
	Where, $\lvert Z\rvert = \sqrt{Z'^2 + Z''^2}$	(2.34)
Admittance	$Y^* = Y' + iY'' = \frac{1}{Z^*}$	(2.35)
	$Y' = \frac{Z'}{Z'^2 + Z''^2}$	(2.36)
	$Y' = \frac{Z''}{Z'^2 + Z''^2}$	(2.37)
AC Conductivity	$\sigma^* = \sigma' + i\sigma'' = \frac{t}{A}\left(\frac{Z' + iZ''}{Z'^2 + Z''^2}\right)$	(2.38)
	$\sigma' = \frac{t}{A}\left(\frac{Z'}{Z'^2 + Z''^2}\right)$	(2.39)
	$\sigma' = \frac{t}{A}\left(\frac{Z''}{Z'^2 + Z''^2}\right)$	(2.40)

Dielectric permittivity	$\varepsilon = \varepsilon^{'} - i\varepsilon^{''} = \frac{1}{i\omega C_0} Y^{*} = \frac{1}{i\omega C_0}\frac{1}{Z^{*}}$	(2.41)
	$\varepsilon^{'} = \frac{1}{\omega C_0}\left(\frac{Z^{''}}{Z^{'2} + Z^{''2}}\right)$	(2.42)
	$\varepsilon^{''} = \frac{1}{\omega C_0}\left(\frac{Z^{'}}{Z^{'2} + Z^{''2}}\right)$	(2.43)
Dielectric Modulus	$M^{*} = M^{'} + iM^{''} = \frac{1}{\varepsilon^{*}} = i\omega C_0 Z^{*}$	(2.44)
	$M^{'} = \omega C_0 Z^{''}$	(2.45)
	$M^{''} = \omega C_0 Z^{'}$	(2.46)

where t = Thickness of the film

A= Cross-sectional area of electrode-electrolyte contact,

$C_0 = \frac{\varepsilon_0 A}{t}$, where, C_0 = Vacuum capacitance and

ε_0 = permittivity of free space = 8.85×10^{-12} F/m.

References

[1] B. L. Papke, M. A. Ratner, and D. F. Shriver, "Vibrational spectroscopy and structure of polymer electrolytes, poly(ethylene oxide) complexes of alkali metal salts," *J. Phys. Chem. Solids*, vol. 42, no. 6, pp. 493–500, 1981, doi: https://doi.org/10.1016/0022-3697(81)90030-5.

[2] P. G. Bruce and C. A. Vincent, "Polymer electrolytes," *J. Chem. Soc. Faraday Trans.*, vol. 89, no. 17, pp. 3187–3203, 1993, doi: 10.1039/FT9938903187.

[3] M. A. Ratner, P. Johansson, and D. F. Shriver, "Polymer Electrolytes: Ionic Transport Mechanisms and Relaxation Coupling," *MRS Bull.*, vol. 25, no. 3, pp. 31–37, 2000, doi: DOI: 10.1557/mrs2000.16.

[4] G. F.M., *Solid Polymer Electrolytes: Fundamentals and Technological Applications*. New York: VCH, 1991.

[5] J. R. MacCallum and C. A. Vincent, Eds., *POLYMER ELECTROLYTE REVIEWS-I*, Elsevier A. Springer, 1987.

[6] P. Prabakaran, R. P. Manimuthu, and S. Gurusamy, "Influence of barium titanate nanofiller on PEO/PVdF-HFP blend-based polymer electrolyte membrane for Li-battery applications," *J. Solid State Electrochem.*, vol. 21, no. 5, pp. 1273–1285, 2017, doi: 10.1007/s10008-016-3477-z.

[7] K. Shahi and J. B. Wagner, "Ionic conduction in KBr-KI mixed crystals," *J. Phys. Chem. Solids*, vol. 44, no. 2, pp. 89–94, 1983, doi: https://doi.org/10.1016/0022-3697(83)90154-3.

[8] D. E. Fenton, J. M. Parker, and P. V. Wright, "Complexes of alkali metal ions with poly(ethylene oxide)," *Polymer (Guildf).*, vol. 14, no. 11, p. 589, Nov. 1973, doi: 10.1016/0032-3861(73)90146-8.

[9] N. K. Karan, D. K. Pradhan, R. Thomas, B. Natesan, and R. S. Katiyar, "Solid polymer electrolytes based on polyethylene oxide and lithium trifluoro- methanesulfonate (PEO–$LiCF_3SO_3$): Ionic conductivity and dielectric relaxation," *Solid State Ionics*, vol. 179, no. 19, pp. 689–696, 2008, doi: https://doi.org/10.1016/j.ssi.2008.04.034.

[10] E. Crawford and B. Bolin, "Arrhenius: From Ionic Theory to the Greenhouse Effect," *Phys. Today*, vol. 50, no. 7, pp. 61–61, Jul. 1997, doi: 10.1063/1.881809.

[11] H.Vogel, "The law of the relationship between viscosity of liquids and the temperature," *Phys. J.*, vol. 22, pp. 645–646, 1921.

[12] G. Tammann and W. Hesse, "The dependence of the viscosity on the temperature of supercooled liquids," *J. Inorg. Gen. Chem.*, vol. 156, no. 1, pp. 245–257, Sep. 1926, doi: 10.1002/zaac.19261560121.

[13] G. S. Fulcher, "Analysis of recent measurements of the viscosity of glasses," *J. Am. Ceram. Soc.*, vol. 8, no. 6, pp. 339–355, Jun. 1925, doi: 10.1111/j.1151-2916.1925.tb16731.x.

[14] M. L. Williams, R. F. Landel, and J. D. Ferry, "The Temperature Dependence of Relaxation Mechanisms in Amorphous Polymers and Other Glass-forming Liquids," *J. Am. Chem. Soc.*, vol. 77, no. 14, pp. 3701–3707, Jul. 1955, doi: 10.1021/ja01619a008.

[15] S. Tabata, T. Hirakimoto, H. Tokuda, M. A. B. H. Susan, and M. Watanabe, "Effects of Novel Boric Acid Esters on Ion Transport Properties of Lithium Salts in Nonaqueous Electrolyte Solutions and Polymer Electrolytes," *J. Phys. Chem. B*, vol. 108, no. 50, pp. 19518–19526, Dec. 2004, doi: 10.1021/jp048370n.

[16] M. H. Cohen and D. Turnbull, "Molecular Transport in Liquids and Glasses," *J. Chem. Phys.*, vol. 31, no. 5, pp. 1164–1169, Nov. 1959, doi: 10.1063/1.1730566.

[17] D. Turnbull and M. H. Cohen, "On the Free-Volume Model of the Liquid-Glass Transition," *J. Chem. Phys.*, vol. 52, no. 6, pp. 3038–3041, Mar. 1970, doi: 10.1063/1.1673434.

[18] D. Turnbull and M. H. Cohen, "Free-Volume Model of the Amorphous Phase: Glass Transition," *J. Chem. Phys.*, vol. 34, no. 1, pp. 120–125, Jan. 1961, doi: 10.1063/1.1731549.

[19] M. H. Cohen and G. S. Grest, "A new free-volume theory of the glass transition*," *Ann. N. Y. Acad. Sci.*, vol. 371, no. 1, pp. 199–209, Oct. 1981, doi: 10.1111/j.1749-6632.1981.tb55661.x.

[20] J. H. Gibbs and E. A. DiMarzio, "Nature of the Glass Transition and the Glassy State," *J. Chem. Phys.*, vol. 28, no. 3, pp. 373–383, Mar. 1958, doi: 10.1063/1.1744141.

[21] G. Adam and J. H. Gibbs, "On the Temperature Dependence of Cooperative Relaxation Properties in Glass-Forming Liquids," *J. Chem. Phys.*, vol. 43, no. 1, pp. 139–146, Jul. 1965, doi: 10.1063/1.1696442.

[22] D. F. Shriver, R. Dupon, and M. Stainer, "Mechanism of ion conduction in alkali metal-polymer complexes," *J. Power Sources*, vol. 9, no. 3, pp. 383–388, Jan. 1983, doi: 10.1016/0378-7753(83)87043-8.

[23] B. L. Papke, "Conformation and Ion-Transport Models for the Structure and Ionic Conductivity in Complexes of Polyethers with Alkali Metal Salts," *J. Electrochem. Soc.*, vol. 129, no. 8, p. 1694, 1982, doi: 10.1149/1.2124252.

[24] P. G. Bruce, Ed., *Solid State Electrochemistry*. Cambridge University Press., 1997.

[25] P. Sharma, "Study of conduction mechanism in PEO-PMMA polymer blend nanocomposite electrolytes," The M.S.University of Baroda, Vadodara.

[26] S. B. Aziz, T. J. Woo, M. F. Z. Kadir, and H. M. Ahmed, "A conceptual review on polymer electrolytes and ion transport models," *J. Sci. Adv. Mater. Devices*, vol. 3, no. 1, pp. 1–17, Mar. 2018, doi: 10.1016/J.JSAMD.2018.01.002.

[27] S. D. Druger, A. Nitzan, and M. A. Ratner, "Dynamic bond percolation theory: A microscopic model for diffusion in dynamically disordered systems. I. Definition and one-dimensional case," *J. Chem. Phys.*, vol. 79, no. 6, pp. 3133–3142, Sep. 1983, doi: 10.1063/1.446144.

[28] S. D. Druger, M. A. Ratner, and A. Nitzan, "Polymeric solid electrolytes: Dynamic bond percolation and free volume models for diffusion," *Solid State Ionics*, vol. 9–10, pp. 1115–1120, 1983, doi: https://doi.org/10.1016/0167-2738(83)90139-X.

[29] M. A. Ratner and A. Nitzan, "East ion conduction: some theoretical issues," *Solid State Ionics*, vol. 28–30, pp. 3–33, 1988, doi: https://doi.org/10.1016/S0167-2738(88)80002-X.

[30] S. D. Druger, M. A. Ratner, and A. Nitzan, "Applications of dynamic bond percolation theory to the dielectric response of polymer electrolytes," *Solid State Ionics*, vol. 18–19, pp. 106–111, 1986, doi: https://doi.org/10.1016/0167-2738(86)90095-0.

[31] A. Nitzan and M. A. Ratner, "Conduction in Polymers: Dynamic Disorder Transport," *J. Phys. Chem.*, vol. 98, no. 7, pp. 1765–1775, Feb. 1994, doi: 10.1021/j100058a009.

[32] A. J. Bhattacharyya, J. Maier, R. Bock, and F. F. Lange, "New class of soft matter electrolytes obtained via heterogeneous doping: Percolation effects in 'soggy sand' electrolytes," *Solid State Ionics*, vol. 177, no. 26–32, pp. 2565–2568, Oct. 2006, doi: 10.1016/J.SSI.2006.02.005.

[33] H. Das Sahu, "Transport properties study and device applications of some polymer

nanocomposite electrolyte systems," Chhattisgarh Swami Vivekanand Technical University Bhilai (India), 2018.

[34] W. Wieczorek, K. Such, H. Wyciślik, and J. Płocharski, "Modifications of crystalline structure of PEO polymer electrolytes with ceramic additives," *Solid State Ionics*, vol. 36, no. 3–4, pp. 255–257, Nov. 1989, doi: 10.1016/0167-2738(89)90185-9.

[35] W. Wieczorek, Z. Florjanczyk, and J. R. Stevens, "Composite polyether-based solid electrolytes," *Electrochim. Acta*, vol. 40, no. 13, pp. 2251–2258, 1995, doi: https://doi.org/10.1016/0013-4686(95)00172-B.

[36] J. Przyluski, M. Siekierski, and W. Wieczorek, "Effective medium theory in studies of conductivity of composite polymeric electrolytes," *Electrochim. Acta*, vol. 40, no. 13, pp. 2101–2108, 1995, doi: https://doi.org/10.1016/0013-4686(95)00147-7.

[37] C.-W. Nan and D. M. Smith, "A.c. electrical properties of composite solid electrolytes," *Mater. Sci. Eng. B*, vol. 10, no. 2, pp. 99–106, Oct. 1991, doi: 10.1016/0921-5107(91)90115-C.

[38] C. Nan, "Effective-medium theory of piezoelectric composites," *J. Appl. Phys.*, vol. 76, no. 2, pp. 1155–1163, Jul. 1994, doi: 10.1063/1.357839.

[39] W. Wang and P. Alexandridis, "Composite Polymer Electrolytes: Nanoparticles Affect Structure and Properties," *Polymers (Basel).*, vol. 8, p. 387, Nov. 2016, doi: 10.3390/polym8110387.

[40] E. Langer, K. Bortel, S. Waskiewicz, and M. Lenartowicz-Klik, "1 - Assessment of Traditional Plasticizers," in *Plastics Design Library*, E. Langer, K. Bortel, S. Waskiewicz, and M. B. T.-P. D. from P.-C. P. E. T. Lenartowicz-Klik, Eds. William Andrew Publishing, 2020, pp. 1–11.

[41] A. Kirkpatrick, "Some Relations Between Molecular Structure and Plasticizing Effect," *J. Appl. Phys.*, vol. 11, no. 4, pp. 255–261, Apr. 1940, doi: 10.1063/1.1712768.

[42] F. W. Clark, "No Title," *Plast. Soc. Chem. Ind. e J. Chem. Ind.*, vol. 60, pp. 225–228, 1941.

[43] W. Aiken, T. Alfrey Jr., A. Janssen, and H. Mark, "Creep behavior of plasticized vinylite VYNW," *J. Polym. Sci.*, vol. 2, no. 2, pp. 178–198, Apr. 1947, doi: 10.1002/pol.1947.120020206.

[44] D. F. Cadogan and C. J. Howick, *Encyclopedia of Chemical Technology*. New York: John Wiley and Sons, 1996.

[45] T. G. Fox and P. J. Flory, "Second-Order Transition Temperatures and Related Properties of Polystyrene. I. Influence of Molecular Weight," *J. Appl. Phys.*, vol. 21, no. 6, pp. 581–591, Jun. 1950, doi: 10.1063/1.1699711.

[46] A. Marcilla and M. Beltrán, "5 - Mechanisms of plasticizers action," G. B. T.-H. of P. (Second E. Wypych, Ed. Boston: William Andrew Publishing, 2012, pp. 119–133.

[47] F. Scholz, *Electroanalytical Methods*. Springer, Berlin, Heidelberg, 2010.

[48] U. Retter and H. Lohse, "Electrochemical Impedance Spectroscopy," in *Electroanalytical Methods.*, F. Scholz., Springer, Berlin, Heidelberg, 2005.

[49] J. Sharma, "Magnesium Ion Conducting Polymer Electrolytes For Solid-State Magnesium Batteries," University of Delhi, Delhi-110007, India, 2016.

[50] A. GUPTA, "EXPERIMENTAL STUDIES ON ION CONDUCTING POLYMER ELECTROLYTES," JAYPEE UNIVERSITY OF ENGINEERING AND TECHNOLOGY, 2013.

[51] A. K. Jonscher, *Dielectric relaxation in solids*. London: Chelsea Dielectrics Press, 1983.

[52] E. Barsoukov and J. R. Macdonald, *Impedance Spectroscopy: Theory, Experiment, and Applications*, 2nd Editio. New Jersey, USA: John Wiley & Sons, Ltd, 2005.

[53] M. Kumar, "Ion Dynamic Studies of Few Sodium and Ammonium salt Containing Polymer Electrolyte Systems," Banaras Hindu University,Varanasi, 2014.

[54] A. K. Bain and P. Chand, *Ferroelectric:Principles and Application*, First. Wiley-VCH Verlag GmbH & Co.KGaA, 2017.

[55] J. W. Schultz, "Dielectric Spectroscopy in Analysis of Polymers," *Encyclopedia of Analytical Chemistry*. 15-Sep-2006, doi: doi:10.1002/9780470027318.a2004.

[56] K. Deshmukh *et al.*, "Chapter 10 - Dielectric Spectroscopy," in *Micro and Nano Technologies*, S. Thomas, R. Thomas, A. K. Zachariah, and R. K. B. T.-S. M. for N. C. Mishra, Eds. Elsevier, 2017, pp. 237–299.

[57] A. N. Papathanassiou, J. Grammatikakis, I. Sakellis, S. Sakkopoulos, E. Vitoratos, and E. Dalas, "Hopping charge transport mechanisms in conducting polypyrrole: Studying the thermal degradation of the dielectric relaxation," *Appl. Phys. Lett.*, vol. 87, no. 15, p. 154107, Oct. 2005, doi: 10.1063/1.2103388.

[58] C. Odin and M. Nechtschein, "Slow relaxation in conducting polymers," *Phys. Rev. Lett.*, vol. 67, no. 9, pp. 1114–1117, Aug. 1991, doi: 10.1103/PhysRevLett.67.1114.

[59] K. S. Cole and R. H. Cole, "Dispersion and Absorption in Dielectrics I. Alternating Current Characteristics," *J. Chem. Phys.*, vol. 9, no. 4, pp. 341–351, Apr. 1941, doi: 10.1063/1.1750906.

[60] A. K. Jonscher, "The 'universal' dielectric response," *Nature*, vol. 267, no. 5613, pp. 673–679, 1977, doi: 10.1038/267673a0.

[61] N. G. McCrum, B.E.Read, and G.Williams, *Anelastic and Dielectric Effects in Polymeric Solids*. New York: Wiley, 1967.

[62] M. PB, M. CT, and R. BOSE, "The role of ionic diffusion in polarisation in vitreous ionic conductors," *Phys. Chem. Glas.*, vol. 13, pp. 171–179, 1972.

[63] I. M. Hodge, M. D. Ingram, and A. R. West, "A new method for analyzing the a.c. behavior of polycrystalline solid electrolytes," *J. Electroanal. Chem. Interfacial Electrochem.*, vol. 58, no. 2, pp. 429–432, 1975, doi: https://doi.org/10.1016/S0022-0728(75)80102-1.

[64] M. Iwamoto, "Maxwell–Wagner Effect BT - Encyclopedia of Nanotechnology," B. Bhushan, Ed. Dordrecht: Springer Netherlands, 2012, pp. 1276–1285.

[65] J. D. Hoffman, "Anelastic and dielectric effects in polymeric solids, N. G. McCrum, B. E. Read, and G. Williams, Wiley, New York, 1967. pp. 617. $25.00," *J. Appl. Polym. Sci.*, vol. 13, no. 2, p. 397, Feb. 1969, doi: 10.1002/app.1969.070130214.

[66] R. Bergman, "General susceptibility functions for relaxations in disordered systems," *J. Appl. Phys.*, vol. 88, no. 3, pp. 1356–1365, Jul. 2000, doi: 10.1063/1.373824.

[67] I. M. Hodge, M. D. Ingram, and A. R. West, "Impedance and modulus spectroscopy of polycrystalline solid electrolytes," *J. Electroanal. Chem. Interfacial Electrochem.*, vol. 74, no. 2, pp. 125–143, 1976, doi: https://doi.org/10.1016/S0022-0728(76)80229-X.

[68] A. K. Jonscher, "Analysis of the alternating current properties of ionic conductors," *J. Mater. Sci.*, vol. 13, no. 3, pp. 553–562, 1978, doi: 10.1007/BF00541805.

[69] B. M. Greenhoe, M. K. Hassan, J. S. Wiggins, and K. A. Mauritz, "Universal power law

behavior of the AC conductivity versus frequency of agglomerate morphologies in conductive carbon nanotube-reinforced epoxy networks," *J. Polym. Sci. Part B Polym. Phys.*, vol. 54, no. 19, pp. 1918–1923, Oct. 2016, doi: 10.1002/polb.24121.

[70] A. K. Jonscher, "Dielectric relaxation in solids," *J. Phys. D. Appl. Phys.*, vol. 32, no. 14, pp. R57–R70, 1999, doi: 10.1088/0022-3727/32/14/201.

[71] K. Funke, R. D. Banhatti, and C. Cramer, "Correlated ionic hopping processes in crystalline and glassy electrolytes resulting in migration-type and nearly-constant-loss-type conductivities," *Phys. Chem. Chem. Phys. (Incorporating Faraday Trans.*, vol. 7, p. 157, Jan. 2005, doi: 10.1039/B414160C.

[72] A. Papathanassiou, I. Sakellis, and J. Grammatikakis, "Universal frequency-dependent ac conductivity of conducting polymer networks," *Appl. Phys. Lett.*, vol. 91, Jun. 2008, doi: 10.1063/1.2779255.

[73] S. Ke, H. Huang, S. Yu, and L. Zhou, "Crossover from a nearly constant loss to a superlinear power-law behavior in Mn-doped $Bi(Mg_{1/2}Ti_{1/2})O_3$–$PbTiO_3$ ferroelectrics," *J. Appl. Phys.*, vol. 107, no. 8, p. 84112, Apr. 2010, doi: 10.1063/1.3386511.